Journal of Physics: Conference Series **645** (2015) 012016 doi:10.1088/1742-6596/645/1/012016

Measurement of Higgs boson properties using the diphoton decay with the ATLAS detector

X. Ruan

School of Physics, University of the Witwatersrand, Johannesburg 2050, South Africa

E-mail: xifeng.ruan@cern.ch

Abstract. The Standard Model Higgs boson like particle was observed in July 2012 by both the ATLAS and CMS collaboration at the LHC. The measurements of the Higgs boson properties are performed in Higgs boson decaying into two photons channel after the discovery. Higgs boson production by the gluon-gluon fusion, the vector boson fusion and in association with a W or Z boson or the top-quark pair are measured in this final state. The multivariate analysis method is applied to extract the Higgs boson in the vector boson fusion enriched category to enhance the signal significance. The couplings of each production modes are measured using $20.3\,\mathrm{fb}^{-1}$ 2012 data taken at center-of-mass energy $\sqrt{s} = 8\,\mathrm{TeV}$ and $4.5\,\mathrm{fb}^{-1}$ 2011 data taken at $\sqrt{s} = 7\,\mathrm{TeV}$ in ATLAS. No significant deviation from the Standard Model prediction is found. The fiducial and differential cross sections of Higgs boson are measured using 2012 data in this final state as well. The distribution of several kinematic variables of the two photons and jets are studied. The results are compared with several theoretical predictions.

Keywords: ATLAS; Higgs boson; Diphoton; Multivariate analysis; Differential; Fiducial

1. Introduction

The Standard Model (SM) Higgs-boson-like particle was observed in 2012 by ATLAS and CMS [1] [2]. After the discovery, the measurements of Higgs properties became important. The Higgs boson coupling strengths in gluon-gluon fusion production, vector boson fusion production (VBF), vector boson associated production (VH) and top production (ttH) were measured. The Higgs boson mass was measured as well. Based on the measured Higgs boson event yields in each bin of the kinematic distribution, the differential cross sections and fiducial cross sections were also measured.

The ATLAS detector [3] is one of the general purpose detectors at the LHC. Its four sub-detectors: the inner detector, the electromagnetic calorimeter, the hadronic calorimeter and the muon spectrometer provide the precise track and energy measurements. Electron, muon, photon and jets are reconstructed in the detector. The measurements were performed by combining the $20.3\,\mathrm{fb}^{-1}$ 8 TeV data taken in 2012 and $4.5\,\mathrm{fb}^{-1}$ 7 TeV data taken from 2011. The differential and fiducial cross section measurements were only using 2012 8 TeV data. The photon energy was re-calibrated in 2013 including implementing the multivariate analysis (MVA) method to improve the identification performance. In the coupling measurement, the multivariate analysis method was also used to improve the sensitivity. The unfolding technique was implemented to extract the Higgs boson kinematic distribution from data to the particle level. The results were compared with several Monte Carlo (MC) prediction using higher order QCD calculation.

2. The Event Selection

In the Higgs boson decaying into the diphoton channel, events are required to have at least two photons. The events must pass the trigger criteria that the transverse energy (E_T) should be larger than 35 GeV and 25 GeV for the leading (highest E_T) and subleading photons, respectively. The photons are restricted to be within the fiducial calorimeter region of $|\eta| < 2.37$ [1] and to exclude the transition region between the barrel and the end-cap calorimeters, $1.37 < |\eta| < 1.56$. The relative p_T: $p_T/m_{\gamma\gamma}$ of the leading and subleading photon should be larger than 0.35 GeV and 0.25 GeV, respectively, in which the $m_{\gamma\gamma}$ is the invariant mass of the two photons. The photons are well identified and isolated. The jets are defined to have $E_T > 25\,\text{GeV}\,(30\,\text{GeV})$ for $|\eta| < 2.4\,(2.4 < |\eta| < 4.5)$.

For the coupling measurement, all of the events which have two photons are categorised into several regions dedicated for different production. It includes the ttH, VH, VBF enriched category. The remaining events are categorised into the bins defined by different conversion configuration or the calorimeter regions. The events in the VBF region are decided using MVA method. The boosted decision tree (BDT) [4] is used. Six kinematic variables are chosen as the inputs to discriminate the signal and background. Each event is given a BDT score and categorised into VBF tight, VBF loose and the other categories, as shown in the left of Fig. 1. The six variables are not correlated to the diphoton invariant mass. They are chosen as below:

- p_{Tt}: Diphoton p_T projected perpendicular to the diphoton thrust axis.
- $\Delta\eta_{jj}$: Pseudo-rapidity separation between the leading two jets. One of the biggest signature of the VBF production mode. The VBF events tend to have two forward jets so that they have larger jet η separation.
- $\eta^{\star}$: $\eta_{\gamma\gamma} - \langle\eta_{jj}\rangle$.
- $\Delta R^{\gamma j}_{\text{min}}$: Minimum ΔR between either the leading/subleading jet and the leading/subleading photon, in which $\Delta\text{R} = \sqrt{\Delta\phi^2 + \Delta\eta^2}$.
- m_{jj}: invariant mass of the leading and subleading jets.
- $\Delta\Phi_{\gamma\gamma jj}$: Azimuthal angle between the diphoton and the two jets.

The training has used POWHEG [5] MC at next-to-next-to-leading order (NNLO) QCD and next-to-leading order (NLO) electro-weak (EW) corrections. The diphoton background sample for the training is simulated by Sherpa [6].

3. The Coupling and Mass Results

In each category, a signal plus background fit is performed on the $m_{\gamma\gamma}$ shape simultaneously. The couplings are parameterised using the signal strength: μ_{ggF}, μ_{VBF}, μ_{VH} and $\mu_{t\bar{t}H}$, defined as the ratio of the measure event yields over the predicted event yields. The results are shown in the right of Fig. 1 [7].

$$\mu_{ggF} = 1.32 \pm 0.38$$
$$\mu_{VBF} = 0.8 \pm 0.7$$
$$\mu_{WH} = 1.0 \pm 1.6$$
$$\mu_{ZH} = 0.1^{+3.71}_{-0.1}$$
$$\mu_{t\bar{t}H} = 1.6^{+2.7}_{-1.8}$$

The mass measurement is performed with the different categorisation. The diphoton events are divided into 10 categories labeled by low or high p_{Tt}, central, forward or transition region,

[1] η is the pseudo-rapidity, defined as $\eta = -\ln[\tan(\theta/2)]$, θ is the angle between the particle momentum and the beam axis.

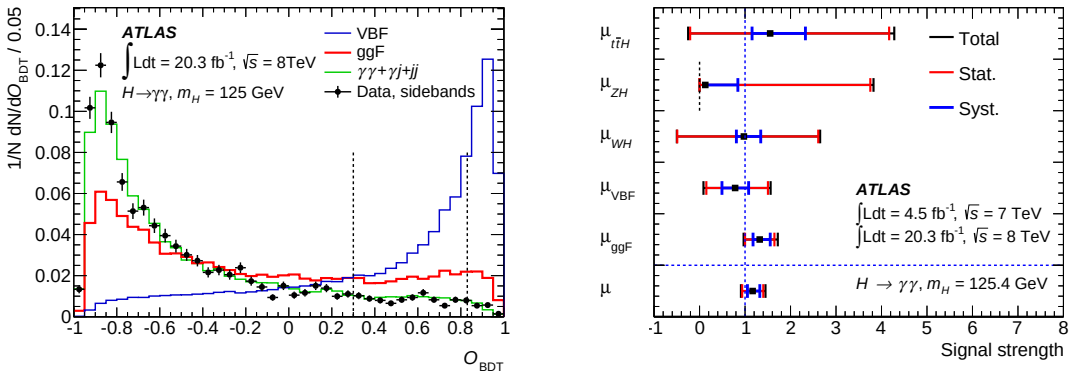

Figure 1. Left: the BDT output of the signal, background and data. The vertical line shows the boundary of categorisations. Right: the measured signal strength in the different Higgs boson production modes [7].

converted or non-converted photons. The unbinned maximum likelihood fit is performed simultaneously in the categories and the 7 TeV and 8 TeV data. The largest systematic uncertainty is the photon energy scale uncertainty. By combining the results from the Higgs boson decaying into four lepton channel, the result is obtained [8]:

$$m_H = 125.36 \pm 0.37(stat) \pm 0.18(syst)\,\text{GeV}$$

4. The Differential and Fiducial Cross Sections

The Higgs boson event yields are measured in each bin of the differential distribution by fitting the invariant mass spectrum. The distributions include the jet activity, Higgs boson kinematics, VBF sensitive variables and spin-CP variable. The variables are listed as below:

- Higgs boson kinematics: $p^T_{\gamma\gamma}$, $|y_{\gamma\gamma}|$
- Jet activity: Jet multiplicity N_{jets}, $p^{j_1}_T$, $|y_{j_1}|$, $p^{j_2}_T$, the scalar sum of jet transverse momenta, H_T
- Spin-CP sensitive variables: $\Delta\phi_{jj}$, $|cos\theta^\star|$
- VBF-sensitive variables: $|\Delta\phi_{\gamma\gamma,jj}|$, $|\Delta y_{jj}|$

The signal yields are corrected for the effects of detector inefficiency and resolution. The results are obtained by using the bin-by-bin unfolding correction factors derived from MC samples. The results are compared with several theoretical predictions describing the Higgs boson+jets activities. The HRes 2.2 [9] calculation is used to provide the inclusive kinematics of the diphoton system via gluon fusion. HRes is accurate to NNLO+NNLL in QCD. The BLPTW (soft-collinear effective theory, NNLO+NNLL 0-jet + NLO+NLL 1-jet cross sections), JetVHeto and MINLO [10] provide predictions for events associated with jets. No significant mismodelling is observed according to the MC prediction. However a small deviation in Higgs p_T distribution is observed, as shown in the left of Fig. 2. The 2015 new data will help to exclude or verify this phenomenon. The jet multiplicity distribution is shown in the right of Fig. 2.

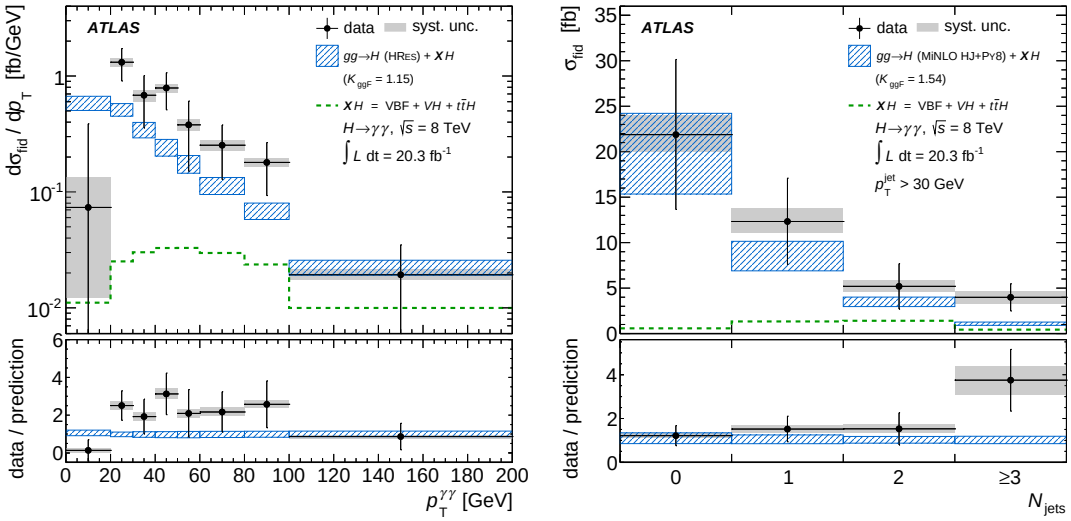

Figure 2. Left: the differential cross section of p_T^H measured in two photon final state. Right: the jet multiplicity distribution. The jet p_T threshold is 30 GeV [11].

The fiducial cross section is also measured in the fiducial range $p_{T\gamma,leading(subleading)}/m_{\gamma\gamma} > 0.35(0.25)$ and 105 GeV$< m_{\gamma\gamma} <$ 160 GeV:

$$43.2 \pm 9.4(stat)^{+3.2}_{-2.9}(syst) \pm 1.2(lumi)\,\text{fb}$$

The cross sections are measured in several fiducial regions as well. They are measured in the inclusive jet bins and the VBF enhanced region. The limits on the cross sections at the 95% confidence level are obtained in the diphoton production with leptons region and the high E_T^{miss} region. The results are compared with several theoretical predictions, as shown in Fig. 3.

5. Conclusions

The Higgs boson mass and coupling were measured after the recalibration of photon energy in ATLAS in 2014. The differential and fiducial cross section were measured as well. No significant deviation from the SM prediction was observed except a small distortion on the Higgs boson p_T distribution. The 2015 Run II data taking is important to verify the measured result, to measure the Higgs boson p_T distribution and to discover the new physics with higher centre mass energy. The multivariate analysis were performed to improve the diphoton analysis. This method will also benefit the 2015 analysis.

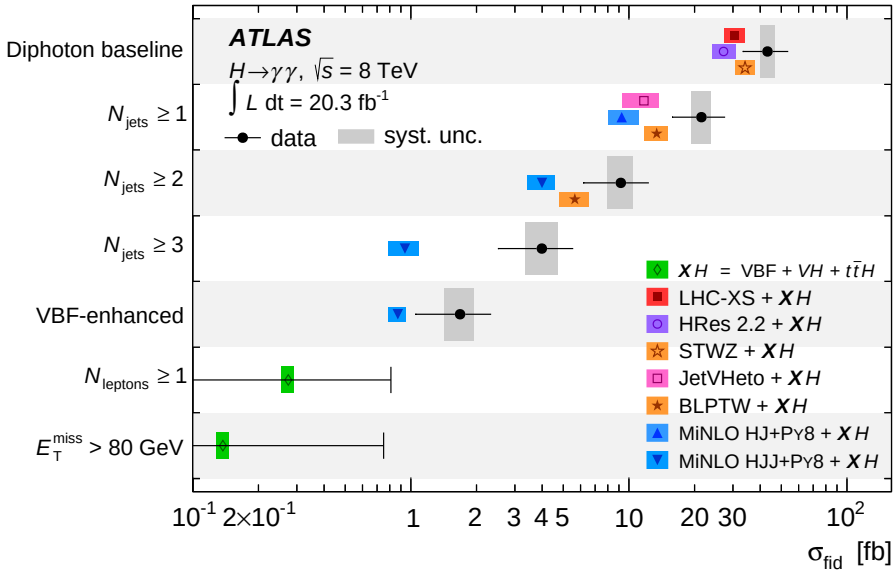

Figure 3. The measured cross sections and cross-section limits for $pp \to H$ in the seven fiducial regions. The intervals on the vertical axis each represent one of these fiducial regions. The data are shown as filled (black) circles. The error bar on each measured cross section represents the total uncertainty in the measurement, with the systematic uncertainty shown as dark grey rectangles. The error bar on each cross-section limit is shown at the 95% confidence level. The width of each theoretical prediction represents the total uncertainty in that prediction. All regions include the SM prediction arising from VBF, VH and ttH, which are collectively labelled as XH [11].

References

[1] ATLAS Collaboration, Phys.Lett. B716 (2012) 1, arXiv:1207.7214[hep-ex]
[2] CMS Collaboration, Phys.Lett. B716 (2012) 30, arXiv:1207.7235 [hep-ex]
[3] ATLAS Collaboration, The ATLAS experiment at the CERN large hadron collider, J.Instrum., 3 (2008)
[4] A. Hoecker, P. Speckmayer, J. Stelzer, J. Therhaag, E. von Toerne, and H. Voss, TMVA 4 (Toolkit for multivariate data analysis with ROOT) Users Guide. 2009
[5] S. Alioli, P. Nason, C. Oleari, and E. Re, JHEP 0904 (2009) 002, arXiv:0812.0578 [hep-ph], P. Nason and C. Oleari, JHEP 1002 (2010) 037, arXiv:0911.5299 [hep-ph]
[6] T. Gleisberg, S. Hoeche, F. Krauss, M. Schonherr, S. Schumann, et al., JHEP 0902 (2009) 007, arXiv:0811.4622 [hep-ph]
[7] ATLAS Collaboration, Phys. Rev. D 90, 112015.
[8] ATLAS Collaboration, Phys. Rev. D 90, 052004.
[9] D. de Florian, G. Ferrera, M. Grazzini, and D. Tommasini, JHEP 06 (2012) 132, [arXiv:1203.6321], M. Grazzini and H. Sargsyan, JHEP 09 (2013) 129, [arXiv:1306.4581].
[10] R. Boughezal, X. Liu, F. Petriello, F. J. Tackmann, and J. R. Walsh, Phys. Rev. D89 (2014) 074044, [arXiv:1312.4535], A. Banfi, P. F. Monni, G. P. Salam, and G. Zanderighi, Phys. Rev. Lett. 109 (2012) 202001,[arXiv:1206.4998], K. Hamilton, P. Nason, and G. Zanderighi, JHEP 10 (2012) 155, [arXiv:1206.3572].
[11] ATLAS Collaboration, JHEP 1409 (2014) 112, arXiv:1407.4222 [hep-ex]